A mountain wind model for assisting fire management

Gary L. Achtemeier•
Center for Forest Disturbance Science
USDA Forest Service, Athens, GA

1. INTRODUCTION

Forestry organizations responsible for managing prescribed fire or controlling wildfire rely on weather forecasts of wind speed and wind direction for planning and allocation of resources. At the locations of fire sites in mountainous areas, winds are highly variable and may differ from winds at distant weather stations or from winds collected at safe sites just a few kilometers from fire lines. These uncertainties in winds can upset plans and place fire fighters in jeopardy. A number of methods to deduce spatial distributions of winds in mountainous terrain exist and it is not the purpose of this article to summarize them.

Among wind analysis methods in use among Forest Service users are mass conservative methods, and Wind Wizard (Forthofer, 2007; Forthofer, J. and B. Butler, 2007). Weise *et al.* (2007) used five methods for deducing wind speeds and directions (including Wind Wizard) for the Esperanza fire that burned 16137 hectares of chaparral and desert scrub vegetation in mountainous terrain in southern California on 26 October 2006. The methods varied in spatial resolution from none to the 100 m resolution of Wind Wizard. The resulting winds were input into the fire spread model, FARSITE (Finney, 1998) for simulating fire spread and compared with fire perimeters deduced from thermal imaging. The results confirmed that accurate wind data are critical if accurate predictions of fire spread are the operational goal.

In addition, there remains a need for a simple, fast, operationally adaptable model to simulate wind flow in mountainous terrain. Achtemeier (2003) derived a fire spread model based on a set of rules and simple equations cast as computer programs solved recursively (Wolfram, 2002). This model demonstrated skill in simulating complex coupled fire-atmosphere interactions and distributions of fire over landscapes. The proof-of-concept of a first-order rule-driven mountain wind model (MWM) is the subject of this paper. The rule and its implementation are described in the next section. Results and discussion of MWM realism follow.

2 . MATERIALS & METHODS

The MWM Rule M1 states that the impact of mountain barriers on wind fields can be described by a pressure function that is solved recursively. The pressure function takes the form,

$$P = C_m(u\frac{\Delta z_s}{\Delta x} + v\frac{\Delta z_s}{\Delta y}) \qquad (1)$$

where,

$$C_m = \frac{C_0 p_0 \Delta x}{RT_0} \qquad (2)$$

where (u, v) are standard horizontal components of the vector wind, z_s is the elevation of the ground, R is the universal gas constant, Δx is the spacing of the model grid ($\Delta x = \Delta y$) and p_0 and T_0 are, respectively, reference pressure and temperature. The coefficient C_0 is a "stability time scale" that ensures convergence of the recursive solution.

Rule M1 was embedded within a modification of the wind model PB-Piedmont (Achtemeier, 2005). PB-Piedmont produces two-dimensional sigma layer-averaged winds draped over a landscape. Maximum resolution within PB-Piedmont determined by the resolution of the USGS national elevation data set is 30 m.

MWM was initialized with Δx ranging from 150 - 600 m, p_0 = 1212.5 mb, T_0 = 300°K. Simulations were done for a layer of depth 100 m draped over complex terrain. Mountains were replaced by the pressure function. However, winds were subjected to mass-weighted corrections. The solutions were not mass conservative.

Initial winds were set to zero. The wind field "spun up" in response to accelerations caused by the sum of the synoptic scale pressure field with the MWM pressure calculated from Equation (1). Objective interpolation of the NWS hourly surface pressures (reduced to sea level) provided the gridded synoptic scale pressure field (Achtemeier, 2005). As acceleration of the wind field is proportional to gradients of the pressure field, the solutions for the wind components are functions derivatives of the wind components – an inherently divergent problem. Thus C_0 is calculated internally in the model to force convergence to a solution,

3. RESULTS & DISCUSSION

The MWM was run as a proof-of-concept

• *Corresponding author address:* Gary L. Achtemeier, Forest Sciences Laboratory, 320 Green Street, Athens, GA 30602; e-mail: gachtemeier@fs.fed.us.

experiment for three diverse mountainous terrains – an isolated mountain in Georgia, an Appalachian ridge in West Virginia, and terrain surrounding the location of the Esperanza fire in southern California. The results for each case are presented and discussed below.

a) Stone Mountain, Georgia

Stone Mountain, GA, is an isolated granite monolith, roughly parabolic in shape with length equal to 2,400 m and width equal to 960 m (Figure 1). The mountain is 500 m in elevation, roughly 235 m above surrounding flat land.

Figure 1. Stone Mountain, GA, looking north. The mountain is surrounded on three sides by lakes. (Image courtesy Google Earth)

A MWM solution for winds blowing from the south is shown in Figure 2. Grid spacing is 150 m. Winds of approximately 8.0 m sec^{-1} at [1] approaching the mountain slow to approximately 2.5 m sec^{-1} at [2] before accelerating to 14.0 m sec^{-1} at [3]. Then the winds decelerate rapidly to approximately 3.0 m sec^{-1} as the air flows down the steep north face of the mountain at [4].

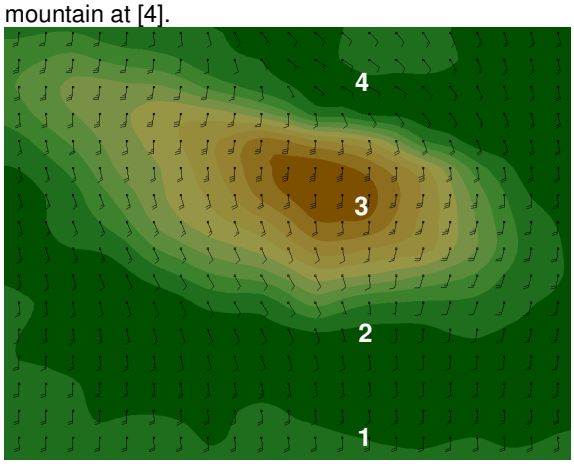

Figure 2. MWM solution for winds blowing from the south over Stone Mountain, GA. Long barb represents wind speed of 5 m sec^{-1} and short barb is 2.5 m sec^{-1}.

The solution bears qualitative resemblance to wind profiles observed at Askervein Hill, Scotland, (Taylor and Teunissen, 1983) (Figure 3 top panel). Wind speeds are presented as ratios with an upwind reference wind speed. The ratios decrease during approach, reaching a minimum of 0.75 at 500m from the peak, then rise to 1.75 at the ridge top followed by sharp decrease to 0.6 downslope.

Figure 3 (lower panel) shows the MWM ratios for winds blowing over Stone Mountain in Figure 2. The drop in the ratio to 0.32 at 400m from the peak is partly explained by wind decreases in the wake of a ridge of low hills upwind from Stone Mountain. The ratio increases to 1.79 at the peak then drops to 0.37 as flow descends down the near shear north face of the mountain.

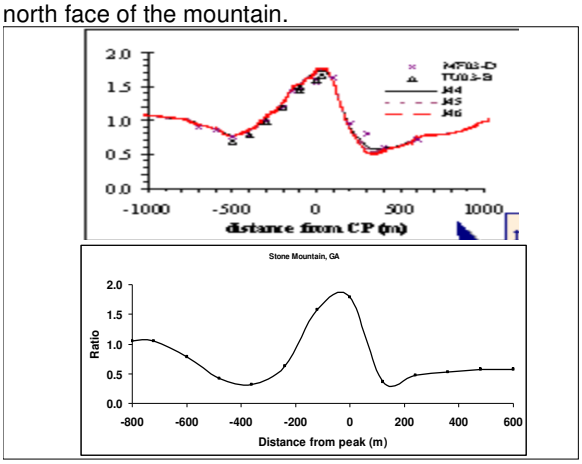

Figure 3. Ratios of wind speed to a reference wind speed for Askervein Hill, Scotland (upper panel) and Stone Mountain, GA (lower panel)

b) Ashwood Ridge, Virginia

The Appalachian Mountains over parts of eastern United States consist of long segmented ridges. Figure 4 shows part of a 28 km unbroken ridge near Ashwood, VA. The ridge rises 400 m above the adjacent valley floors. An airport (KHSP) with a weather station is located on top of the ridge.

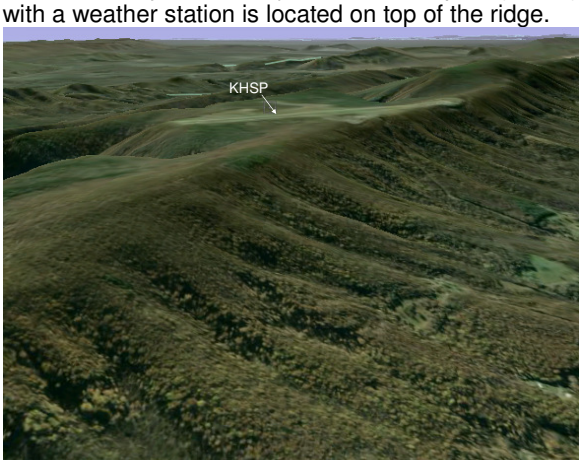

Figure 4. Part of a 400 m high ridge near Ashwood, VA. (Image courtesy Google Earth)

MWM was set up with a 600 m grid. Winds

were simulated from 00 GMT 26 October 2006 through 00 GMT 30 October 2006. Figure 5 shows the first order solution at 2315 LST 8 March 2006. Typical of all solutions is the tendency for MWM to turn the winds to blow over the ridge. Model winds in the valleys are blowing almost parallel to the ridge but with a small component toward the ridge from the south. Note how the wind directions shift to blow more normal to the ridge axis with increased speed. After crossing the ridge, winds shift again to blow nearly parallel with the ridge. Winds speeds also decrease.

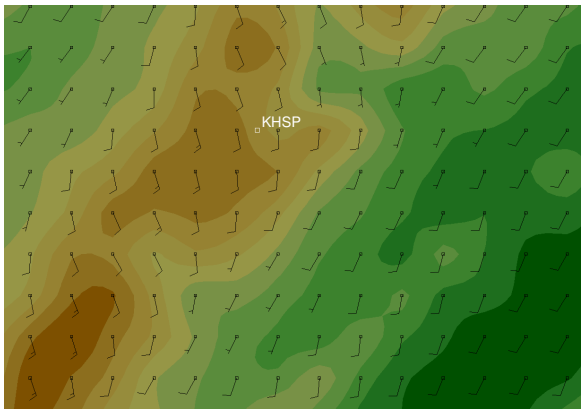

Figure 5. Airflow over Asheville Ridge as simulated by MWM for 2315 LST, 8 March 2006.

When the wind direction was parallel to the ridge, the winds at ridge top blew from that direction. However, when the winds blew from a direction not parallel to the ridge, the ridge top winds blew with a strong cross-ridge component. The black line in Figure 6 shows the behavior of wind direction over a five day period at KHSP. The magenta line shows the first order solution by MWM. During the first day, observed winds had a stronger west component than did the MWM winds based on objective analyses of the pressure data. Thus the terrain forcing turned winds to blow from the west whereas the model turned winds to blow from the south.

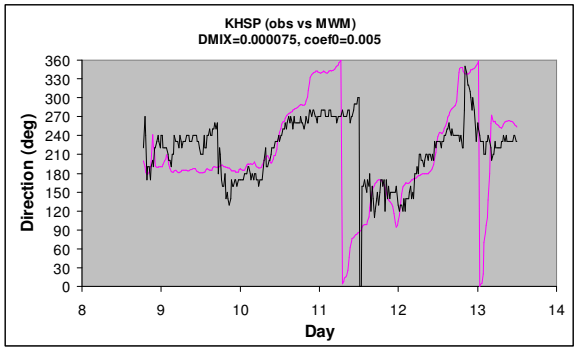

Figure 6. Wind directions at the top of Ashwood Ridge from 8-13 March 2006.

The model wind directions were in approximate agreement with observations during the second and fourth days. During the third day, objective analyses of the pressure field caused winds to shift through north - wind directions not observed.

c) Esperanza Fire, California

In October 2006, the Esperanza wildfire consumed 16137 hectares (39,000 acres) of chaparral and desert scrub vegetation in mountainous terrain approximately 50 km east of Riverside, CA, (Weise *et al*., 2007). Figure 7 shows terrain features that impacted winds during the fire. Terrain rose sharply from a flat valley of 500 m elevation to a rugged plateau that rose gradually from roughly 1000 m. A nearby mountain peaked at 1300 m. A range of higher mountains to the left of the image rose to 3200 m.

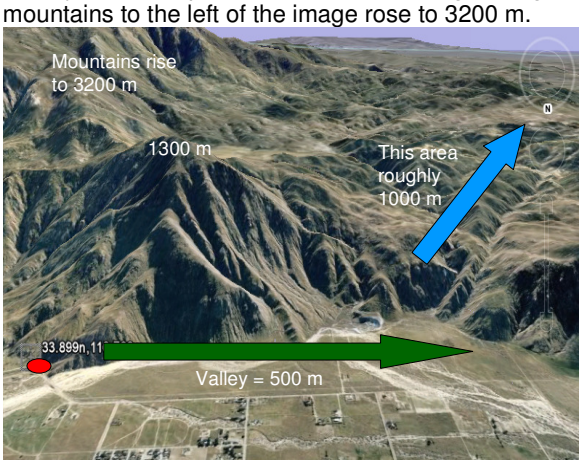

Figure 7. Site of the Esperanza fire looking south. Fire start location is given by the red ellipse. (Image courtesy Google Earth)

The Esperanza fire started at the base of the 1300 m mountain at midnight local standard time (17 GMT) 26 October 2006 (red ellipse)and spread up the mountain while also being spread to the west by strong east winds blowing down the valley (green arrow). After having spread up the steep slopes at the edge of the valley, the fire was found in strong winds blowing from the northeast (blue arrow). These winds blew the fire up drainages with catastrophic effects. The combination of east winds on the valley floor and northeast winds over higher terrain was a major factor in the fire spread history of the Esperanza fire.

The MWM was set up with a 600 m grid that included the area of the fire, the valley and surrounding mountains out to 50 km from the fire. Surrounding NWS weather stations provided pressure observations needed for MWM. The objective was to determine the magnitude of impact of Rule M1 on winds transitioning from low to high terrain.

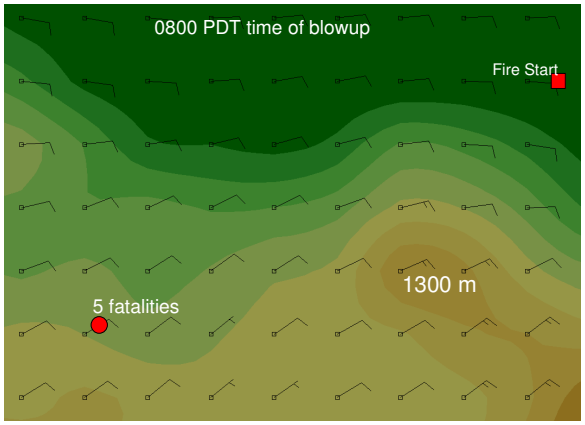

Figure 8. MWM simulated winds at 0800 LST 26 October 2006 for the domain of the Esperanza fire defined roughly by the blue arrow in Figure 8. North is at the top of the figure. The valley is the dark green area at the top of the figure and the 1300 m mountain is brown shaded. Wind barbs represent 5 m sec^{-1} (10 knots).

Figure 8 shows the wind field at 0800 LST (looking north) for a subset of the model domain that includes areas most impacted by the Esperanza fire. The 1300 m mountain in Figure 8 is identified by the brown shaded area. Winds in the valley (dark green area at the top) near the fire start (red square) are blowing from the east. The blocking effect of the 1300 m mountain is a factor in turning the winds to blow from the northeast at higher elevation. Wind speeds increased with increasing elevation. Winds blowing in the valley at approximately 5 m sec^{-1} increased to greater than 10 m sec^{-1} over highest ground.

Figure 9 shows how well MWM simulated the onset of the Santa Anna winds at a weather station located at Banning Airport approximately 8.8km west of the ignition site. MWM Wind directions (top panel) show an abrupt shift from 310 degrees to 080 degrees at approximately -4.0 h BI (before ignition) and continuing until -2 h BI. MWM winds then blew steadily from 85-90 degrees. Wind observations (squares) show a wind shift occurring between -4.7 h and -3.7 h BI. MWM wind directions were in good agreement with observations thereafter.

The wind speeds (lower panel) show that MWM consistently underestimated wind speed by a factor of approximately 1.5. This underestimation was not unexpected as MWM was run from the pressure field calculated from hourly reports from standard National Weather Service weather stations surrounding the fire. Gradients of the final pressure field calculated from the hourly pressure data were determined by station spacing. No allowances were made for the blocking effect of the surrounding mountains which would have increased pressure gradients locally.

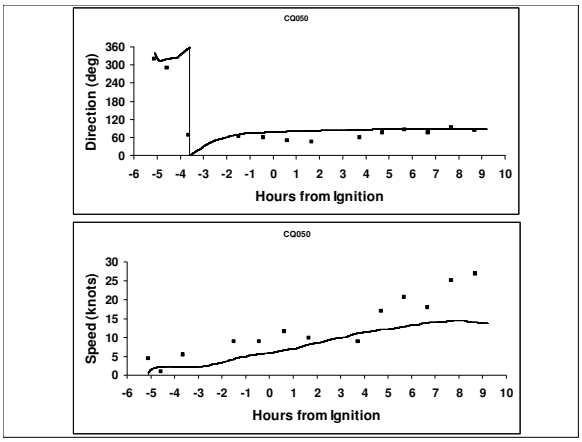

Figure 9. Comparison of MWM winds with observed winds from Banning Airport - wind direction (top panel) and wind speed (bottom panel).

4 . CONCLUSION

The Mountain Wind Model is a work in progress. The three cases described illustrate that Rule M1 produces reasonable first-order effects of the impacts on the wind field by mountainous terrain. The results are for 100 m layer averaged winds draped over complex terrain. For the cases studied, MWM approximated wind directions reasonably well but underestimated wind speeds for the Esperanza case. Underestimation of the strength of the synoptic scale pressure gradient in the mountains accounts for reduced wind speeds.

Because of the simplicity of Rule M1, the MWM in its current state, should produce inaccurate and unrealistic wind fields for the following conditions;

1) Density currents such as drainage flows,
2) Turbulent circulations under high winds,
3) Flows at higher terrain where pressure observations currently used lose validity,
4) Light winds dominated by thermally-induced circulations,
5) Stable temperature strata.

An application of MWM winds to fire spread modeling for the Esperanza Fire in Southern California is presented as a poster.

5. REFERENCES

Achtemeier, G.L., 2003: “Rabbit Rules” – An application of Stephen Wolfram’s “new kind of science” to fire spread modeling. Extended abstract. Fifth Symp. Fire and Forest Meteor., Orlando, FL, Amer. Meteor. Soc.

Achtemeier, G.L., 2005: Planned Burn – Piedmont. A local operational numerical meteorological model for tracking smoke on the ground at night: Model development and sensitivity tests. Int. J. Wildland Fire, 14, 85-98.

Finney, M.A., 1998. FARSITE: Fire Area Simulator--Model Development and Evaluation. *USDA Forest Service Res. Paper RMRS-RP-4,* Rocky Mountain Research Station, Ft. Collins, Colorado.

Forthofer, J.M. 2007 (In prep.) Modeling wind in complex terrain for use in fire spread prediction. Fort Collins, CO: Colorado State University. (Expected completion 2007)

Forthofer, J. and B. Butler. 2007: Differences in Simulated Fire Spread Over Askervein Hill Using Two Advanced Wind Models and a Traditional Uniform Wind Field. In: Butler, B. W.; Cook, W., comps. 2007. The fire environment—innovations, management, and policy; conference proceedings. 26-30 March 2007; Dest in, FL. Proceedings RMRS-P-46. Fort Collins, CO: U.S. Department of Agriculture, Forest Service, Rocky Mountain Research Station. 000 p. CD-ROM.

Taylor, P.A.; Teunissen, H.W. 1983. Askervein '82: Report on the September/October 1982 Experiment to study boundary layer flow over Askervein, South Uist. MSRB-83-8. Downsview, Ontario, CAN: Atmospheric Environment Service.

Weise, D. R., S. Chen, P. J. Riggan, F. M. Fujioka. 2007: Using high-resolution weather data to predict fire spread using the farsite simulator—a case study in california chaparral. Extended abstract. Seventh Symp. Fire and Forest Meteor., Bar Harbor, ME. Amer. Meteor. Soc. 10 pp.

Wolfram, S., 2002: A New Kind of Science. Wofram Media, Inc., 1197 pp.